

Novel Photon-Counting CT Improves Myeloma Bone Disease Detection

Released: September 6, 2022

At A Glance

- New CT technology paired with AI offers superior detection of bone disease associated with multiple myeloma.
- The photon-counting detector CT with deep learning noise reduction detected more lytic lesions relative to conventional CT.
- Photon-counting detector CT could make a difference in the staging of disease, potentially impact therapy choice, and ultimately, patient outcomes.

OAK BROOK, Ill. — New CT technology paired with artificial intelligence (AI)-based noise reduction offers superior detection of bone disease associated with multiple myeloma at lower radiation doses than conventional CT, according to a new study published in *Radiology*, a journal of the Radiological Society of North America (RSNA).

The new technology, known as photon-counting detector CT, debuted in the clinic in 2021 after decades of development. By directly converting individual x-ray photons into an electric signal, photon-counting detector CT can decrease the detector pixel size and improve the image's spatial resolution.

[download photo](#)



Francis Baffour, M.D.

“Additionally, photon-counting CT has demonstrated much better dose efficiency than standard CT, which allows for acquisition of ultra-high-resolution images of large areas of the body,” said study lead author Francis Baffour, M.D., diagnostic radiologist at the Mayo Clinic in Rochester, Minnesota.

This potential for improved image quality in whole-body low-dose scans inspired Dr. Baffour and colleagues to study the technology in people with multiple myeloma, a disease that forms in a type of white blood cell found in the bone marrow called a plasma cell. Bone disease characterized by areas of bone destruction known as lytic lesions is found in approximately 80% of multiple myeloma patients.

The International Myeloma Working Group recommends low-dose, whole-body CT to evaluate associated bone disease. Much less is known about photon-counting detector CT in this setting.

Dr. Baffour and colleagues compared photon-counting detector CT with conventional low-dose, whole-body CT in 27 multiple myeloma patients, median age 68 years. The patients underwent whole-body scans with both types of CT and two radiologists compared the images.

“We felt this was a prime example to showcase the ultra-high-resolution of photon-counting CT at low scanning doses,” Dr. Baffour said.

The researchers also applied a deep learning AI technique developed at Mayo Clinic's CT Clinical Innovation Center to reduce the noise in the very sharp photon-counting images. CT noise refers to an unwanted change in pixel values in the image, often loosely defined as the grainy appearance on cross-sectional imaging. The photon-counting detector CT with deep learning noise reduction demonstrated improvement in visualization and detected more lesions relative to conventional CT.

“We were excited to see that not only were we able to detect these features of multiple myeloma disease activity more clearly on the photon-counting scanner,” Dr. Baffour said, “with deep learning denoising techniques that allowed us to generate thinner image slices, we were able to detect more lesions than on the standard CT.”

The researchers hope to conduct follow-up studies on patients with multiple myeloma precursor states to see if photon-counting detector CT finds bone lesions that would upstage these patients to active multiple myeloma.

“Our excitement as scientists and radiologists in these results stems from our realization that this scanner could make a difference in the staging of disease, potentially impact therapy choice, and ultimately, patient outcomes.”

They also want to look at photon-counting detector CT in other instances in which low-dose protocols are beneficial, for instance, in pediatric or pregnant patients or screening applications.

“Already there are ongoing studies to determine how low we can go with scanning doses while still obtaining diagnostic CT images,” Dr. Baffour said. “So, there is much on the horizon and so much potential for photon-counting detector CT in clinical care.”

Dr. Baffour credited his colleagues, Cynthia McCollough, Ph.D., and Joel Fletcher, M.D., directors of Mayo Clinic's CT Clinical Innovation Center, for their work in developing clinical applications of photon-counting detector CT.

“Photon-counting Detector CT with Deep Learning Noise Reduction to Detect Multiple Myeloma.” Collaborating with Drs. Baffour, McCollough and Fletcher were Nathan R. Huber, Ph.D., Andrea Ferrero, Ph.D., Kishore Rajendran, Ph.D., Katrina N. Glazebrook, M.D., Ch.B., Nicholas B. Larson, M.S., Ph.D., Shaji Kumar, M.D., Joselle M. Cook, M.B.B.S., Shuai Leng, Ph.D., and Elizabeth R. Shanblatt, Ph.D.

For patient-friendly information on whole-body CT, visit [RadiologyInfo.org](https://www.rsna.org/radiologyinfo).

Images (JPG, TIF):

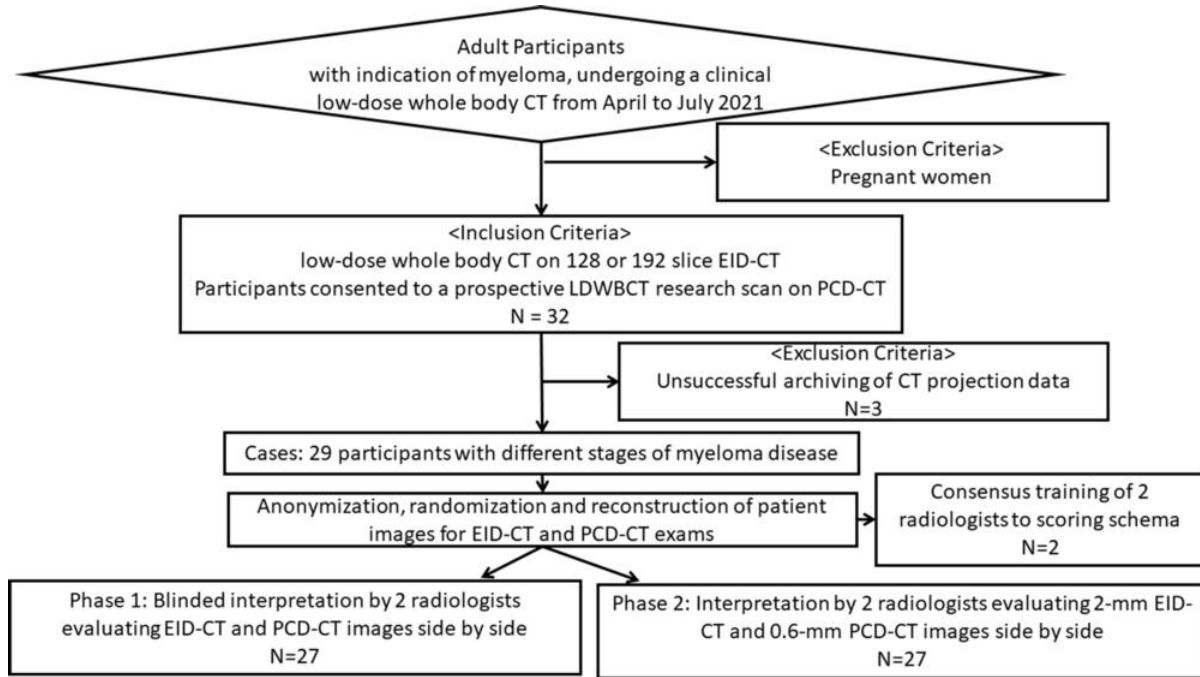


Figure 1. Study inclusion and exclusion flowchart. EID = energy-integrating detector, PCD = photon-counting detector.

[High-res \(TIF\) version](#)

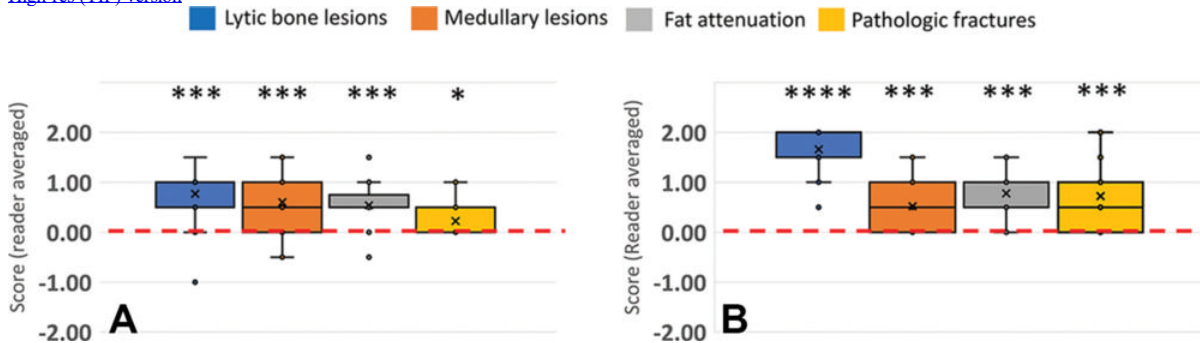


Figure 2. Box and whisker plots of reader-averaged scores for reader assessments in (A) phase 1 and (B) phase 2. Reader-averaged scores are presented on the vertical axis. A neutral score of zero is indicated by the horizontal dashed red line. A score of +1 (-1) indicates preference for the photon-counting detector (PCD) CT (energy-integrating detector [EID] CT) images, with no change in diagnostic confidence. A score of +2 (-2) indicates improved diagnostic confidence for the PCD CT (EID CT) images. Symbols above each assessment indicated Holm-adjusted significance level under a two-sided one-sample Wilcoxon rank sum test. * $P < .05$, ** $P < .01$, *** $P < .001$, **** $P < .0001$.

[High-res \(TIF\) version](#)

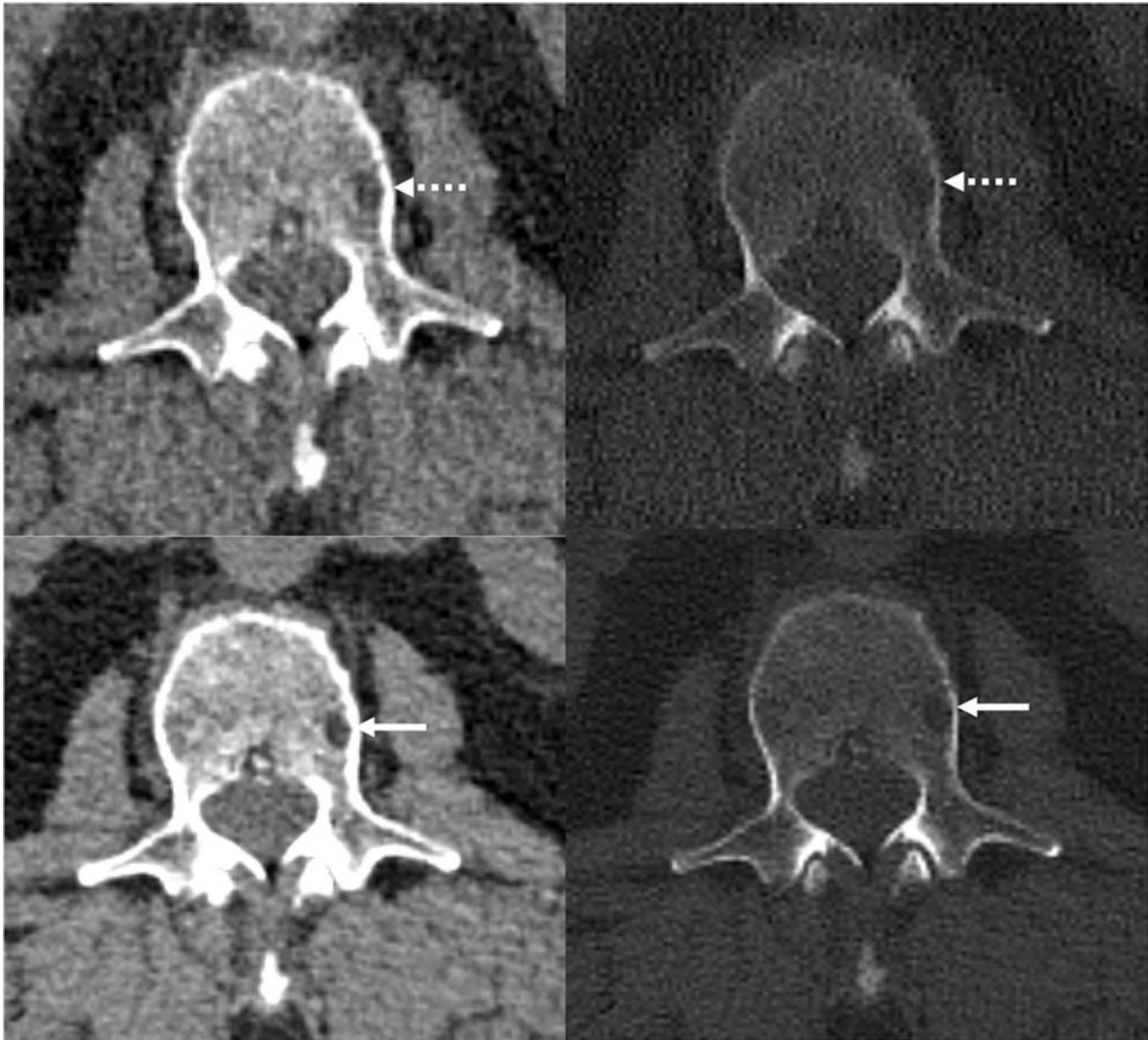


Figure 3. Reference protocol (top) and evaluated protocol (bottom) images in a 74-year-old man with multiple myeloma. The soft tissue reconstruction is shown, whereas the right column is the bone reconstruction. A lytic bone lesion in the L3 vertebral body is more conspicuous on the noncontrast-enhanced axial photon-counting detector CT reconstruction images (bottom; solid arrows) compared with the noncontrast-enhanced axial energy-integrating detector CT reconstruction images (top; dashed arrows).
[High-res \(TIF\) version](#)

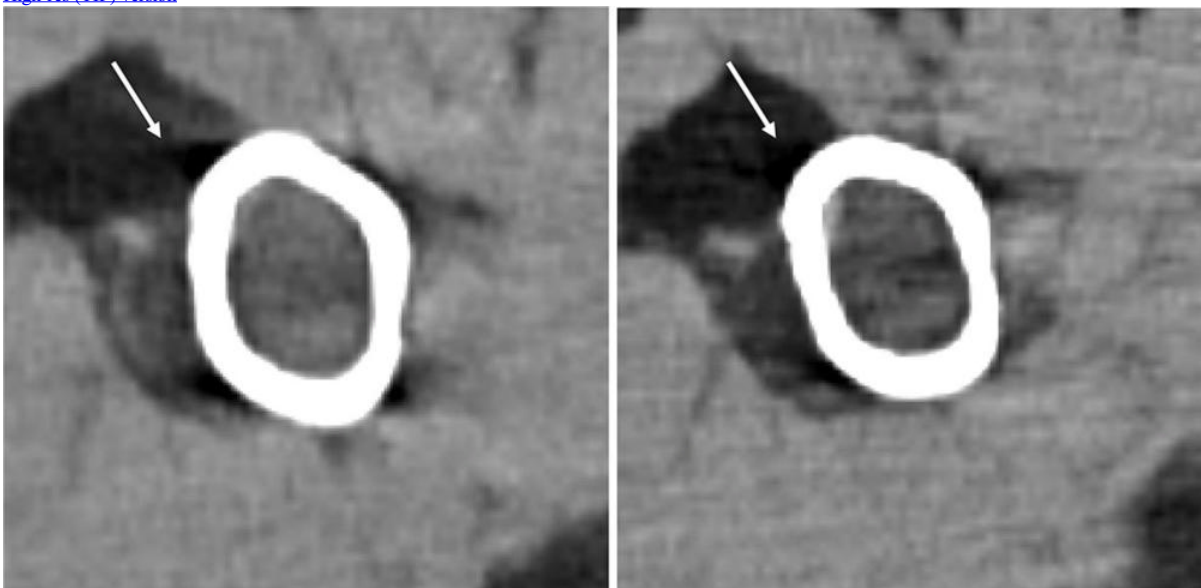


Figure 4. Images in a 71-year-old man with relapsed multiple myeloma, after autologous stem cell transplant, who was administered single-agent daratumumab maintenance therapy. Foci of intramedullary hyperattenuation in the left proximal humerus with macroscopic internal fat suggested fatty

metamorphosis of a multiple myeloma lesion after therapy. The degree of fat infiltration is better appreciated on the noncontrast-enhanced axial photon-counting detector (PCD) CT image (right), compared with the noncontrast-enhanced axial energy-integrating detector CT image (left). Beam hardening artifact (arrows), notably along the anterior cortex of the proximal humerus, is reduced on the PCD CT image.

[High-res \(TIF\) version](#)



Figure 5. Images in a 71-year-old man with multiple myeloma. Lytic lesions (dashed arrows) within a thoracic vertebral body and the left iliac wing are more conspicuous on the noncontrast-enhanced axial photon-counting detector (PCD) CT image (middle; solid arrows) compared with noncontrast-enhanced axial energy-integrating detector CT image (left). With 0.6-mm Br76 noncontrast-enhanced axial PCD CT reconstruction images (right), more lesions were detected (arrowheads).

[High-res \(TIF\) version](#)

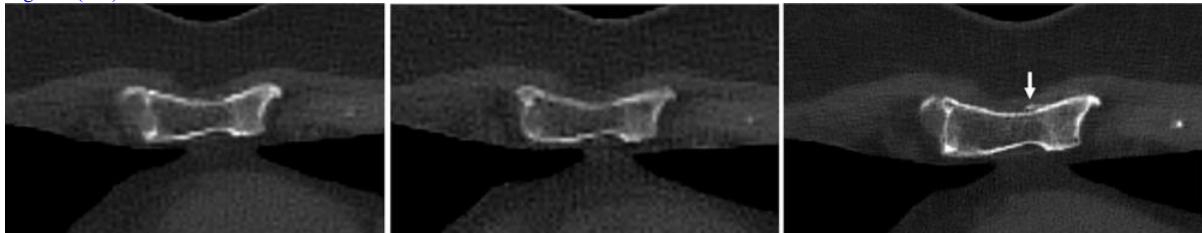


Figure 6. Images in a 60-year-old woman with multiple myeloma. Two-millimeter noncontrast-enhanced axial energy-integrating detector CT image (left), 2-mm noncontrast-enhanced axial photon-counting detector (PCD) CT image (center), and noncontrast-enhanced axial 0.6-mm PCD CT image (right) show representative pathologic myeloma-induced healing pathologic fracture through the lower sternum. Cortical irregularity is evident on all three reconstruction images; however, the associated callus is only visible on the 0.6-mm PCD CT reconstruction image (right; arrow).

[High-res \(TIF\) version](#)

Resources:

[Study abstract](#)